THE JOURNAL OF GENE MEDICINE
J Gene Med 2004; **6**: 574–583.
Published online 8 March 2004 in Wiley InterScience (www.interscience.wiley.com). **DOI:** 10.1002/jgm.486

RESEARCH ARTICLE

Excision of *Sleeping Beauty* transposons: parameters and applications to gene therapy

Geyi Liu[1,2]
Elena L. Aronovich[1,3]
Zongbin Cui[1,2,4]
Chester B. Whitley[1,3]
Perry B. Hackett[1,2,5]*

[1]*Department of Genetics, Cell Biology and Development and The Institute of Human Genetics, University of Minnesota, Minneapolis, MN 55455, USA*

[2]*The Arnold and Mabel Beckman Center for Transposon Research, University of Minnesota, Minneapolis, MN 55455, USA*

[3]*Department of Pediatrics, University of Minnesota, Minneapolis, MN 55455, USA*

[4]*Institite of Hydrobiology, Chinese Academy of Sciences, Wuhan, P.R. China*

[5]*Discovery Genomics, Inc., Minneapolis, MN 55413, USA*

*Correspondence to:
Perry B. Hackett, Discovery Genomics, Inc., 614 McKinley Place NE, Minneapolis, MN 55413, USA.
E-mail:
perryh@discoverygenomics.net

Received: 13 March 2003
Revised: 27 May 2003
Accepted: 27 June 2003

Abstract

A major problem in gene therapy is the determination of the rates at which gene transfer has occurred. Our work has focused on applications of the *Sleeping Beauty* (SB) transposon system as a non-viral vector for gene therapy. Excision of a transposon from a donor molecule and its integration into a cellular chromosome are catalyzed by SB transposase. In this study, we used a plasmid-based excision assay to study the excision step of transposition. We used the excision assay to evaluate the importance of various sequences that border the sites of excision inside and outside the transposon in order to determine the most active sequences for transposition from a donor plasmid. These findings together with our previous results in transposase binding to the terminal repeats suggest that the sequences in the transposon-junction of SB are involved in steps subsequent to DNA binding but before excision, and that they may have a role in transposase–transposon interaction. We found that SB transposons leave characteristically different footprints at excision sites in different cell types, suggesting that alternative repair machineries operate in concert with transposition. Most importantly, we found that the rates of excision correlate with the rates of transposition. We used this finding to assess transposition in livers of mice that were injected with the SB transposon and transposase. The excision assay appears to be a relatively quick and easy method to optimize protocols for delivery of genes in SB transposons to mammalian chromosomes in living animals. Copyright © 2004 John Wiley & Sons, Ltd.

Keywords footprint; mouse liver; *Tc1/mariner*; terminal repeats; transposition

Introduction

Tc1/mariner transposons are a large family of DNA transposable elements. They are widespread in nature and can be found in virtually all animal phyla [1,2]. Recently, we reconstructed a synthetic Tc1-like vertebrate transposon system called *Sleeping Beauty* (SB) from inactive salmonid fish elements by a comparative phylogenetic approach [3]. In mammalian cells, the SB transposon system is an order of magnitude more efficient than other Tc1 family members tested [4]. Since its discovery, SB has been used in a wide range of vertebrate systems [5] for functional genomics [6–8], germ-line transgenesis [4,6,9], and somatic integration [10–12]. Its higher efficiency compared to other DNA-based transposable elements, its ability to accommodate large genetic cargoes [5,13], and its presumed safety compared to viral vectors make SB a potentially powerful tool for human gene therapy.

The SB transposon system consists of two parts – the transposon, consisting of inverted terminal repeats (ITRs), and the SB transposase that catalyzes the mobilization of the transposon. Like other members of the *Tc1/mariner*

transposon family, SB transposons are mobilized via a cut-and-paste mechanism (Figure 1A). There are two major steps involved in transposition, the excision of the transposon from the donor site and the integration of the transposon into the target site [2]. Excision from the donor site involves staggered, double-stranded DNA breaks at each side of the transposon, which result in a small number of nucleotides at the termini of the transposon being left behind [2,14]. The majority of *Tc1/mariner* transposons integrate into TA-dinucleotide base pairs in a fairly random manner [8,9,15]. As a result of the staggered cut at the TA target sites, the transposons are flanked by TA-dinucleotides on both sides after integration (Figure 1B), a phenomenon called target-site duplication [2,3].

The ITRs of the current SB transposon came from a single *Tc1*-like element from a salmonid, *Tanichthys albonuibes* – referred to as *T*. *T* has two inverted repeats (IRs) at its termini and two 'direct repeats' (DRs) within each IR (Figure 1A). The outer DRs, Lo and Ro, are located at the left and right termini of the transposon, respectively, and the inner DRs, Li and Ri, are located further inside the transposon. Both DRs contain binding sites for SB transposase [3] and the middle 18 bp within the DRs have been suggested to comprise a minimal core sequence for transposase binding [16]. Both the outer and inner DRs are required for efficient transposition [3], but they are not interchangeable, indicating that their roles in transposition are different [16].

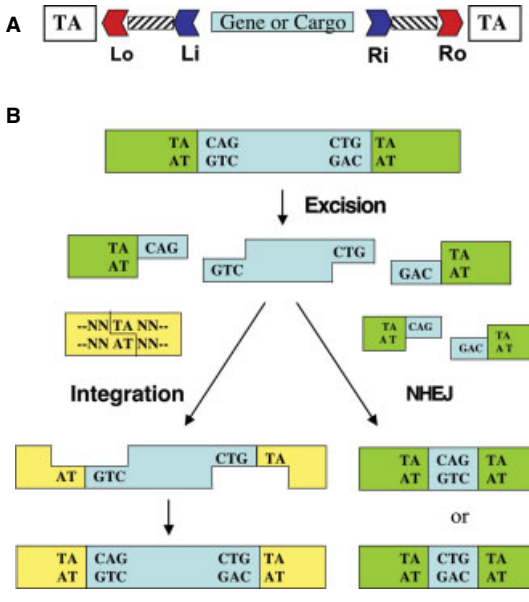

Figure 1. The *Sleeping Beauty* (SB) transposon and its transposition. (A) Structure of the terminal repeats of the SB transposon. The DRs of the ITRs are designated by arrowheads and are labeled according to their positions in the transposons used in this study. The boxed TAs flanking the transposon result from duplication of the original TA insertion site. (B) "Cut-and-paste" mechanism of SB transposition revised from Luo *et al.* [14] and Plasterk *et al.* [2]. The two major steps involved in transposition, excision and integration of a transposon are shown. The two broken ends at the donor sites, joined together by non-homologous end-joining (NHEJ) enzymes encoded by the host, leave a footprint at the donor site

PCR-based excision analysis has been used to detect excision from a chromosomal location by SB transposase [4,7,9,14]. However, this method is not suitable for studying the mechanism of transposition because the excision is limited to a particular transposon and a particular donor site in the chromosomal position. Plasmid-based excision assays, on the other hand, are more versatile and easier to perform [18,19]. Hence, we developed a plasmid-based excision assay for the SB transposon system to study the different steps of transposition in more detail and found a correlation between the excision rate and the transposition rate. Using this assay, we analyzed the footprints of SB in tissue-cultured cells as well as in zebrafish embryos and mice. The results of these studies directed design of a better transposon as well as led to the development of a method for determining transposition from a plasmid in organs of mice. This latter assay should be extremely useful for optimizing SB-mediated transposition reactions in mammals as a step towards harnessing the transposon for gene therapy. In such procedures, a gene contained in a transposon vector is prepared at high concentrations in a plasmid that is then delivered by any of several methods to a target organ. As a result, the sequence of the donor plasmid can serve as a common site for monitoring the excision step of the transposition reaction.

Materials and methods

Plasmids

The maps and sequences for plasmids pCMVSB (also called pSB10) and pSB10-ΔDDE, which contain an active and inactive transposase gene, respectively, and pT/neo which contains a transposon [3] as well as pT/HindIIIneo (Adam Dupuy, unpublished) can be found through our website [20]. We name pT/HindIIIneo variants by the DRs that are in their left and right IRs. All variant pT/HindIIIneo constructs were made by PCR-mediated, site-directed mutagenesis described previously for LoLi–LiLo, RoRi–RiRo, LiLi–RiRo and LoLo–RiRo [16]. Mutagenic primers *Sac*I + Lo and *Bam*HI + Ro were used to amplify complete variant transposons on pT/HindIIIneo. After digesting with *Sac*I and *Bam*HI, the PCR fragments were ligated into the *Sac*I/*Bam*HI vector fragment of pT/HindIIIneo. All constructs were confirmed by sequencing.

Mutagenic primers we used are listed below with specific mutations underlined:

*Sac*I + Lo (AAA): TTGGAGCTCGGTACCCTAAAATTGAAGTC

*Sac*I + Lo (CAA): TTGGAGCTCGGTACCCTACAATTGAAGTC

*Sac*I + Lo (AAG): TTGGAGCTCGGTACCCTAAAGTTGAAGTC

*Bam*HI + Ro (AAA): AGCTAGAGGATCCCCTAAAATTGAAGTCG

*Bam*HI + Ro (CAA): AGCTAGAGGATCCCCTACAATTGA-AGTCG
*Bam*HI + Ro (AAG): AGCTAGAGGATCCCCTAAAGTTGA-AGTCG
*Bam*HI + Ro (CC): AGCTAGAGGATCCCCCCCAGTTGAA-GTCG
*Sac*I + Lo (GG): TTGGAGCTCGGTACCCGGCAGTTGAA-GTC

Plasmid-based excision analysis

Excision in HeLa cells: 500 ng pT/neo or pT/HindIIIneo mutation constructs were co-transfected with 100 ng pCMVSB (or pSB10-ΔDDE) into 3×10^5 HeLa cells. Four days post-transfection, cells were collected and lysed in 200 µl lysis buffer [50 mM KCl, 10 mM Tris-HCl (pH 8.3), 2.5 mM $MgCl_2$, 10 mM EDTA, 0.45% (w/v) NP40, 0.45% (w/v) Tween-20, 100 µg/ml Proteinase K] and incubated at 55 °C for 2–3 h followed by 95 °C for 20 min to inactivate the Proteinase K. For temporal analyses, 5 µl of lysate were added to the PCR mixture [1 × NH_4 PCR buffer, 3 mM $MgCl_2$, 0.2 mM dNTP, 10 pmol forward and reverse primer each, 0.5 µl Biolase, buffer and enzyme from Bioline USA]. The PCR conditions were as follows: 94 °C for 5 min, 60 cycles of (94 °C 30 s, 64 °C 30 s, 72 °C 20 s), followed by 72 °C for 10 min. Five µl of 1/50 dilution of the above PCR product were used for the second round PCR using nested primers and 1.5 mM $MgCl_2$; the composition of the PCR mixture was otherwise the same. Nested PCR was performed at 94 °C for 5 min, 35 cycles of (94 °C 30 s, 64 °C 30 s, 72 °C 5 s), followed by 72 °C for 10 min. For pT/neo, only one round of PCR was performed and gave products of about 582 bp. Primers were:

o-lac-L: 5′-GGCTGGCTTAACTATGCGGCATCAG-3′
o-lac-R: 5′-GTCAGTGAGCGAGGAAGCGGAAGAG-3′

For pT/HindIIIneo and its mutation constructs, nested PCR gave products of about 316 bp. Primers were:

1st round: F1-ex: 5′-CCAAACTGGAACAACACTCAAC-CCTATCTC-3′
o-lac-R: 5′-GTCAGTGAGCGAGGAAGCGGAAGAG-3′.
2nd round: KJC031: 5′-CGATTAAGTTGGGTAACGCCAG-GGTTT-3′
i-lac-R: 5′-AGCTCACTCATTAGGCACCCCAGGC-3′.

Excision in zebrafish embryos: 25 ng/µl pT/neo was co-injected with 25 ng/µl SB mRNA into one-cell-stage zebrafish embryos. SB transposase mRNA was synthesized by *in vitro* transcription using the Message Machine large-scale *in vitro* transcription kit (Ambion). The injection volume for each embryo was 1–3 nl. Twenty-four hours after injection, single embryos were lysed in 50 µl lysis buffer [10 mM EDTA, 10 mM Tris-HCl (pH 8.0), 200 µg/ml Proteinase K] as described [18,19] for 3 h at 50 °C, followed by 20 min incubation at 95 °C to inactivate the Proteinase K; 2 µl of embryo lysate were used for PCR. The program used for PCR was as follows: 94 °C 5 min, 30 cycles of (94 °C 30 s, 67 °C 30 s), 25 cycles of (94 °C for 30 s, 67 °C for 30 s, 72 °C for 5 s) followed by 72 °C for 10 min.

Excision in mouse liver: DNA was isolated from 8 mm^3 frozen liver specimens using the Puregene DNA purification kit (Gentra Systems, Minneapolis, MN, USA). PCR was performed in two rounds of amplification. PCR I was carried out in a 50-µl reaction mixture containing 1 µg DNA, 5% DMSO, 5% glycerol, 10 pmol each forward and reverse primer, a 0.2 mM concentration of each dNTP, 1× PCR buffer A (Invitrogen, Carlsbad, WI, USA), and 5U *Taq* DNA polymerase (Promega, Madison, WI, USA). PCR conditions were: 95 °C for 5 min followed by 45 cycles of (95 °C, 40 s, 58 °C, 30 s, 72 °C for 1 min) with the final extension of 5 min at 72 °C. A 10-µl aliquot of the primary PCR product was used for secondary amplification in a 100-µl reaction with nested primers (10 µm concentration) and the same cycling conditions except that the number of cycles was 35. The expected size of the amplified excision product was approximately 456 bp. The primers used for the excision assay were outside left and right ITRs. The primer sequences were:

FP1: 5′-TGACGTTGGAGTCCACGTTC-3′
RP1: 5′-GGCTCGTATGTTGTGTGG-3′
FP2: 5′-CTGGAACAACACTCAACCCT-3′
RP2: 5′-CACACAGGAAACAGCTATGA-3′.

Detection and quantification of the PCR product

The excision PCR products were separated on 3% low-melt gels (GenePure Sieve GQA agarose, ISC Bioexpress) and stained with 50 µg/ml ethidium bromide. For better resolution and quantification, PCR products were separated on 6% polyacrylamide gels and stained with 1 : 10 000 dilution of SYBR green I (Molecular Probes, Inc.) for 45 min. The gels were scanned with a Storm phosphor imager (Molecular Dynamics) at 850 V in the blue fluorescence mode to visualize the bands. To standardize the input total plasmid DNA for each PCR, a 1/5000 dilution of initial lysate was used to amplify a segment of the ampicillin-resistance gene on both pCMVSB and input pT transposon plasmid (depending on the experiment, it could be pT/HindIIIneo, one of the mutants, or pT/neo). These products were separated on 1% agarose gel and stained with 50 µg/ml ethidium bromide. The intensity of each band was measured in arbitrary increments of density units (integrated optical density, IOD) using Gel-Pro analyzer imaging software (Media Cybernetics). The background was corrected using the filtered profile method, as instructed in the manual.

The relative excision activity of the mutated transposon constructs was derived from their standardized IOD, i.e., the IOD of the excision band divided by the relative input template. The relative excision activity is indicated as a percentage of the excision activity of the control transposon pT/HindIIIneo, for which a standard curve

derived from the ratio of the different dilutions of the transposon was constructed.

Footprint sequencing

To sequence the footprint, the PCR products were gel-extracted (for mutations with low excision activity, reamplified with the nested PCR), cloned into the TOPO TA cloning vector (Invitrogen) and sequenced by the Advanced Genetics Analysis Center at the University of Minnesota.

Transposon delivery to mouse liver

The transposon-containing plasmid pT/CAGGS-GUSB (transposon) and the transposase-expressing plasmid pCMVSB were used to assay transposition in adult mouse tissues (Aronovich *et al*., manuscript in prep.). The transposon contains an expression cassette for the GUSB gene to restore activity to mutant mice deficient in β-glucuronidase activity. The mucopolysaccharidosis (MPS) type VII mice (B6.C-H-2bml/ByBir-gus^{mps}) were obtained from Jackson Laboratories (Bar Harbor, ME, USA) and maintained in the AAALAC-accredited specific pathogen-free mouse facility at the University of Minnesota. The plasmids were injected into the tail vein of homozygous 12–16-week-old MPS VII mice using a 3-ml latex-free syringe with a 271/2G needle. The hydrodynamics-based procedure was performed as described [21,22]. Each mouse received plasmid DNA in lactated Ringer's solution in a total volume equal to 10% of body weight. 25 µg of a single preparation of transposon pT/CAGGS-GUSB were injected either alone ('Treatment Group 1'), or with pCMVSB at 10 : 1 transposon/transposase molar ratio ('Treatment Group 2'). 37.5 µg DNA were injected into all mice with pBluescript plasmid as a 'filler'; the sham treatment control group of MPS VII mice was injected with pBluescript alone. All injections were performed only once. The mice were euthanized 1-week post-injection, livers were harvested and frozen at −80 °C. Excision assays were performed as described above.

Results

Assay for the excision step of transposition

We developed and used the excision assay first in HeLa cells where we co-transfected the transposon plasmid pT/neo and the transposase-expressing plasmid pCMVSB (Figure 2). Three days after transfection, the plasmids in the cell lysate were used as templates for PCR. Using primers flanking the donor sites, we detected excision by amplifying a PCR product that corresponded to the size of a rejoined vector after the excision of the transposon. As shown in Figure 3A, a PCR product of

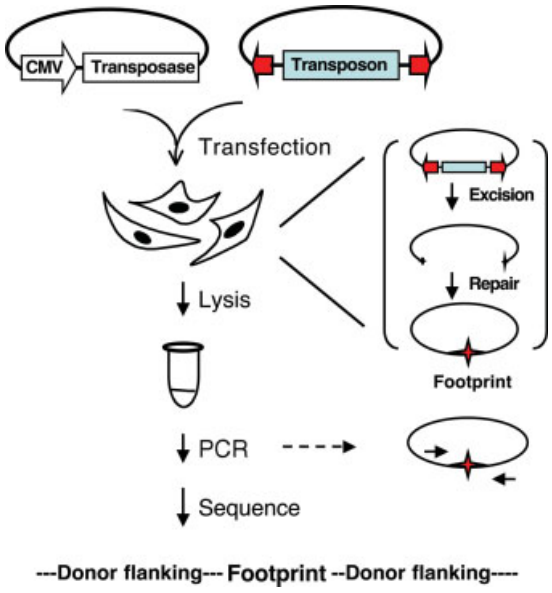

Figure 2. Schematic of the excision assay. Plasmids containing a transposon and CMVSB transposase were co-transfected into HeLa cells. Four days post-transfection, cell lysates were obtained and used for PCR with primers flanking the donor sites. The PCR products were sequenced to determine the footprints of the excision. The procedure is shown on the left and the state of the transposon and its excision product is shown on the right

approximately 582 bp was amplified in cell lysates from a pCMVSB and pT/neo co-transfection. The PCR product appeared to be specific to SB excision because neither pSB-ΔDDE, which has a mutated catalytic domain, the transposon plasmids alone, nor the transposase plasmids alone, produced the 582-bp product. Figure 3B shows the accumulation of the excision products over several days. Excision products were detectable 18 h after transfection and their levels continued to rise through 89 h after transfection. In subsequent experiments, we collected samples at 72 h for quantification of excision events under different conditions. Figure 3C shows the same excision assay carried out in zebrafish embryos. We co-injected transposon plasmids and SB mRNA as the source of the transposase. Extracts of 24-h embryos were used for analysis of excision by PCR. As with the cell cultures, excision was evident only in the presence of SB transposase, which supports our previous findings [9].

Footprints of SB excision

We cloned and sequenced the excision PCR products to study the footprints left by the transposons. Table 1 shows the summary of the footprint sequences acquired from HeLa cells and zebrafish embryos. The two flanking sides of the transposon had footprints of varying lengths that we categorized in one of three ways – canonical footprint, non-canonical footprint, gap/insertion. Canonical footprints had 7-bp sequences TACAGTA or TACTGTA conforming to the model illustrated in Figure 1B (5-bp insertions of either CAGTA or CTGTA following

Table 1. Footprint sequences from HeLa cells and zebrafish embryos

Systems	Category	Left-flanking	Footprint	Right-flanking	Events
HeLa cells	Canonical footprints	TTCGAGCTCGGTACCC	TA CAG TA	GGGGATCCTCTAGAGT	4
		TTCGAGCTCGGTACCC	TA CTG TA	GGGGATCCTCTAGAGT	2
	Non-canonical footprints	TTCGAGCTCGGTACCC	T– –-G TA	GGGGATCCTCTAGAGT	3
		TTCGAGCTCGGTACCC	TA ––– TA	GGGGATCCTCTAGAGT	2
		TTCGAGCTCGGTACCC	TA C–– TA	GGGGATCCTCTAGAGT	1
		TTCGAGCTCGGTACCC	T– –TG TA	GGGGATCCTCTAGAGT	1
		TTCGAGCTCGGTACCC	TA C–– –A	GGGGATCCTCTAGAGT	1
	Gaps	(82-bp deletion)	––– –G TA	GGGGATCCTCTAGAGT	1
		(67-bp deletion)	–– ––– ––	(89bp deletion)	1
	Insertions	TTCGAGCT	TGCATGTGGGAGGTTTTTTC	GGATCCTCTANAGT	1
Zebrafish embryos	Canonical footprints	TTCGAGCTCGGTACCC	TA CTG TA	GGGGATCCTCTAGAGT	5
		TTCCAACNCGGTACCC	TA CAG TA	GGGAATCCTCTAGAGT	4
	Gaps	(17bp deletion)	–– ––– ––	(19bp deletion)	1

Excision sites were sequenced using primers outside the transposon. Short lines indicate the lost nucleotides. Footprint sequences are organized in several categories. Canonical footprints have 7-bp sequences of TACAGTA or TACTGTA, conforming to the model illustrated in Figure 1B. Non-canonical footprints have small deletions in the 7-bp canonical sequence. Gaps have larger deletions in either or both sides of the flanking sequence as indicated.

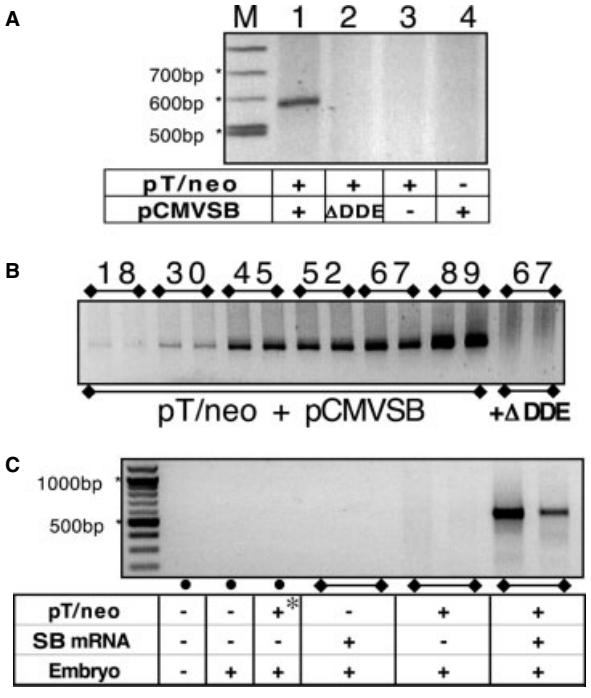

Figure 3. PCR analysis of transposon excision from plasmids in HeLa cells (A and B) and in zebrafish embryos (C). (A) Plasmids with transposons and CMVSB transposase (pT/neo and pCMVSB) were co-transfected into the HeLa cells. Cell lysate was obtained for nested-PCR using primers outside the transposon. ΔDDE is a transposase without a catalytic domain. (B) Time-course accumulation of excision products from HeLa cells. Hours post-transfection are marked on top of the gel. Each time point is represented by two separate transfections. The marker lane (M) on the left of the gels in A and C is a 100-bp ladder (New England Biolabs). (C) SB mRNA was co-injected into one-cell-stage zebrafish embryos with plasmids containing a transposon (pT/neo). Twenty-four hours after microinjection, lysates from single embryos were used for PCR analysis. Two different embryos were used in the last three categories. *: pT/neo plasmids mixed with embryo lysate were used as template in this case

the insertion TA site). Non-canonical footprints had small deletions in the 7-bp canonical sequences. In the case of HeLa cells, deletions were usually 2–3 bp. Gaps had large deletions (17–89 bp) on either or both sides of the flanking sequences. In one case, we observed a 20-bp insertion of unknown origin between the two flanking sites. Most of the footprints in zebrafish embryos were canonical footprints, whereas the footprints in HeLa cells consisted of similar percentages of canonical and non-canonical footprints.

Excision activity correlates to transposition activity

A preliminary study suggested that the excision activities correlate to the transposition activity [16]. We examined this hypothesis by measuring the excision activity of IR/DR mutations shown to have different transposition rates to evaluate its validity. To quantify the levels of excision, we generated a set of standards using dilutions of the excision lysate of the original pT/HindIIIneo. As the control for the total input template, we used the amplification of a segment in the backbone of both pT and pCMVSB plasmids. For each gel scan, we first standardized the intensity of the excision bands (in arbitrary increments of density units, IOD) by dividing the IOD of the excision bands by the relative amount of total input plasmid. A standard curve was generated from the standardized IOD values of the amplification products resulting from dilutions of the standard pT/HindIIIneo. The relative excision activity for each reaction was calculated as a percentage of the pT/HindIIIneo activity. Figure 4 shows one example of a gel scan and the quantification of the excision footprints. We compared these relative excision activities with the earlier reported transposition rates measured by a transposition assay [16]. In this assay, transposon-mediated chromosome integration was indicated by the increase in the number of G418-resistant colonies, and the transposition rate was measured as the percentage of the pT/HindIIIneo activity. The comparisons of the activities of transposition and excision are summarized in Table 2. Mutations with high excision activities correlated with high transposition activities

and mutations with low excision activities correlated with low transposition activities. Although transposition activities varied between parallel experiments, the relative excision activities approximated transposition rates within the uncertainties of our measurements, suggesting that excision can be used as an indicator of transposition efficiency and thereby for improvement of the SB system.

Use of the excision assay to improve the SB transposon system

The outer and inner DRs have different roles in excision and transposon can be excised efficiently only at the outer DRs [16]. These results suggested that it is not the location but the differences in sequence between Lo and Li that gives them different functional roles. Comparison of the Lo and Li sequences showed that there are two discrete regions in Lo that are different from Li, regions I and II (Figure 5A). To determine which region is critical for excision, we made mutations in each and tested whether the excision activity was impaired.

We focused on two positions in region I because the model in Figure 1 predicts that the C in the first position (C1) and the G in the third position (G3) at the tip of Lo and Ro demarcate the staggered cuts. These positions, which are the same on the left and right IRs, should thus be vital to the overall interaction between transposon and transposase in this region. If true, changing the nucleotides at these two positions should affect this interaction and cause reduced excision activity. Figure 5B is a detailed analysis of positions C1 and G3 in Lo and Ro. In Lo, when we changed either C1 or G3, excision activity was reduced to 11 and 18%, respectively, indicating that both C1 and G3 contribute to excision activity. The double mutation at both +1 and +3 reduced excision activity to below the limit of detection. The same mutations were made in Ro and the effects were similar, indicating that these positions have the same functions on both sides. These data suggest that the nucleotides in the first and the third positions at the termini of the outer DRs in region I are critical for excision.

We tested the requirement for region II by mutating three out of the five terminal basepairs (TTAAG to GGGAG). Comparison of Figure 5C lanes 1 and 2 indicated that the exact sequence of region II was not critical for excision because mutating these three base pairs did

Table 2. Comparison of relative excision activity and relative transposition rates

Constructs	Relative excision activity	Relative transposition rate
LoLi – RiRo + ΔDDE	nd	4% (1%)*
LoLi – RiRo	100%	100% (30%)
RoRi – RiRo	42%	29% (6%)
LoLi – LiLo	95%	101% (30%)
LiLi – RiRo	nd	4% (1%)*
LoLo – RiRo	46%	43% (23%)

Relative excision activities were measured as described in Figure 4. The relative transposition rates were determined as described in Cui *et al*. [16]. Transposition rates are averages of four to seven independent transfections, numbers in parentheses show the 95% confidence interval. nd, non-detectable; *, background level of colony number. LoLiRiRo is pT/Hindillneo.

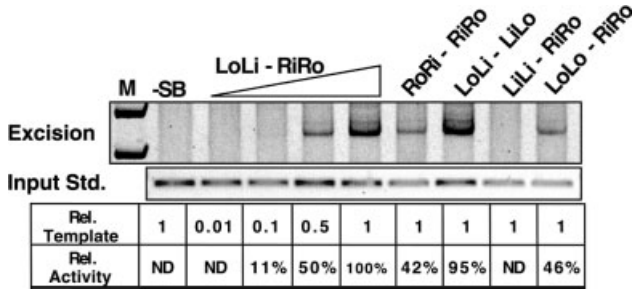

Figure 4. Quantification of relative excision activity in HeLa cell excision assay. Excision levels of four IR/DR mutations were measured relative to the activity of LoLi–RiRo (the pT/HindIIIneo transposon). The top gel shows excision PCR products run on a 6% polyacrylamide gel stained with SYBR green I. The lower gel shows PCR amplification of a segment of the backbone of pT/neo and pCMVSB (or pSB10-ΔDDE) as an input control for the total plasmid in the lysate. The relative excision abundance was measured as a ratio of the band intensity of the excision PCR products to that of the amplification of the segment on the plasmid backbone. "Rel. template" indicates the relative amount of the input lysate. Relative excision activity ("Rel. activity") is indicated as a percentage of control activity using the ratio for each mutation compared to a standard curve derived from the ratio of the different dilutions of the original pT/HindIIIneo activity. ND, non-detectable

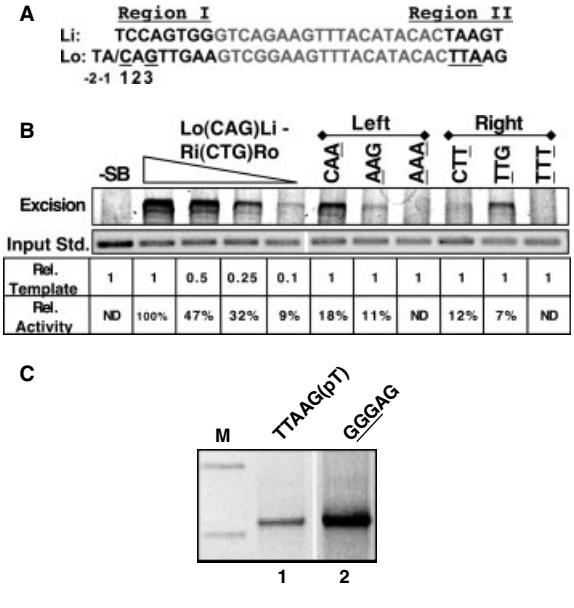

Figure 5. Terminal nucleotides in the outer DRs are important for excision. (A) Sequence comparison of Lo and Li. Mutated sequences in regions I and II are underlined. (B) Mutations in region I at the first and third positions at the terminus of Lo are underlined. Lo(CAG)Li–Ri(CTG)Ro indicate the pT/HindIIIneo transposon. Quantification of the excision activity is as described in Figure 4. ND, non-detectable. (C) Mutations in region II wherein three out of the five terminal base pairs (TTAAG to GGGAG) were changed

not reduce excision activity. Instead, the excision activity seems to have been increased. The band intensity for the GGGAG mutation construct was eight times more intense than that of the pT (TTAAG), which exceeded the limit of our detection method. This trend persisted in repeated experiments, leading us to incorporate these mutations in the next generation of improved transposon DNA (unpublished).

TA-dinucleotides flanking the transposon affect excision

The TA-dinucleotides flanking the transposon are of special interest. SB transposons insert only into TA-dinucleotides, where a target-site duplication event leads to TA flanks on both sides of the transposon [1]. This raised the question of whether there is a functional requirement for TA in excision. We examined this question by replacing the TA-dinucleotides flanking the transposon. We found that excision can still occur when only one flanking TA is present, although activity is dramatically reduced. When we replaced both TAs, the excision rate was reduced to below the limit of detection (Figure 6A). These results show that the TAs flanking the transposon are strongly involved in excision and confirm our earlier finding of their importance in the overall transposition process [16]. We were able to acquire complete footprints from the two mutation constructs lacking TA on one side (Figure 6B). The footprints showed that when GG replaced the TA outside the outer DR, the substitution remained in the footprints (underlined GGs in Figure 6B).

Use of the excision assay to evaluate SB activity in adult animals

The SB transposon system has been used for gene transfer into mice as a model for use in human gene therapy [10–12]. However, evaluating the efficacy of transposition is difficult because delivery of transposons to many different cells of an organ results in integration events in different sites of various chromosomes. Hence, we examined whether the excision assay could be used for this purpose.

We used the hydrodynamic delivery method of Liu *et al*. [21] and Zhang *et al*. [22] to deliver an SB transposon to MPS VII mice that were completely deficient in lysosomal hydrolase β-glucuronidase [23]. The transposon plasmid we constructed contained an expression cassette for β-glucuronidase CAGGS-GUSB (Aronovich *et al*., in preparation). Two groups of mice were injected with pT/CAGGS-GUSB: Treatment Group 1 received only the transposon-containing plasmid, Treatment Group 2 was co-injected with pCMVSB plasmid at a molar ratio of 10 : 1 transposon/transposase. As in zebrafish, we detected excision events only when both transposon and transposase were injected (Figure 7). The PCR bands were excised from the gel for cloning and sequencing as described in the previous section. The predominant band of 456 bp yielded eight readable sequences, seven of which gave canonical footprints of TAC(A/T)GTA (Table 4), similar to those found in zebrafish embryos and mouse ES cells (Table 3) and one of which appeared to be a transposition event using an alternative TA excision site. Another six events were sequenced from smaller, minor bands that showed deletions of various sizes and nucleotide sequences that indicated illegitimate

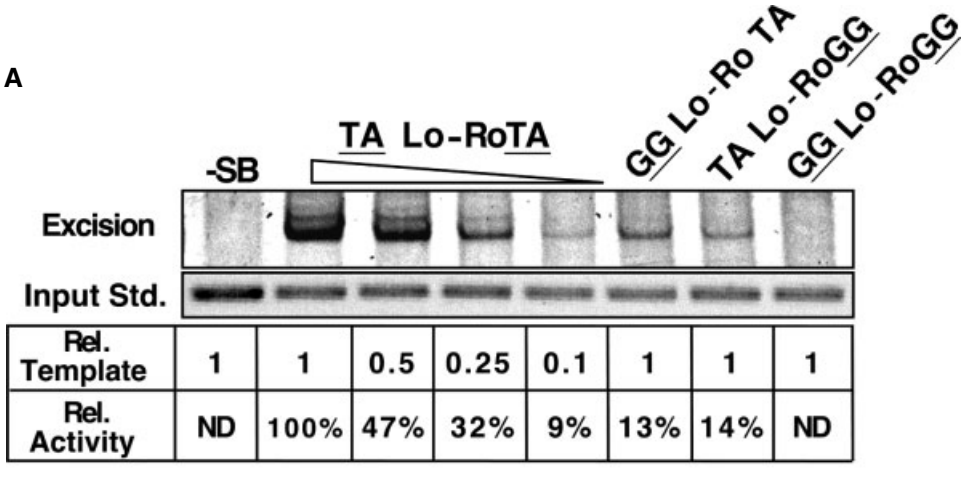

Rel. Template	1	1	0.5	0.25	0.1	1	1	1
Rel. Activity	ND	100%	47%	32%	9%	13%	14%	ND

Figure 6. Effect of TA-dinucleotides on excision. (A) Excision analysis of TA mutations on either side and both sides of the transposon. TA Lo-RoTA indicates the pT/HindIIIneo transposon. Mutations are underlined. (B) Sequences of the excision site of the mutated transposons. The footprints are underlined. ND, non-detectable

Table 3. Comparison of SB footprints in different systems

	Canonical footprint	Non-canonical footprint missing			Gaps/ Insertions	Total events	Reference
		1 bp	2 bp	3 bp			
HeLa cell cultures	35%	0	18%	29%	18%	17	This study
Zebrafish embryos	96%	0	0	0	4%	25	This study and [g]
Mouse spermatids	0	31%	44%	0	25%	16	[4]
Mouse ES cells	85%	0	0	8%	8%	13	[14]
Mouse Livers	88%	0	0	0	12%	8	This study

Table 4. Footprint sequences from mouse livers

	Left-flanking	Footprint	Right-flanking	Events
Major	**Band of expected size ~456 bp**			
Canonical	GACTCACTATAGGGCGAATTGGAGCTCGGTACCC	**TA CAG TA**	GGGGATCCTCTAGCTAGAGT	6
footprints	GACTCACTATAGGGCGAATTGGAGCTCGGTACCC	**TA CTG TA**	GGGGATCCTCTAGCTAGAGT	1
Gaps	GACTCACTA- - - - - - - - - - - - - - - - - - - -	- - - - - - -	- - - - - - - - - - - TAGAGT	1
Minor	**Bands of smaller size**			
	(82 bp deletion)	- - - - - - -	(36 bp deletion)	1
Deletions	(87 bp deletion)	- - - - - - -	(40 bp deletion)	1
	(96 bp deletion)	- - - - - - -	(76 bp deletion)	1
Random	54 bp upstream of left TA, sequence continues at right ITR.			1
insertion	78 bp upstream of left TA			1
	82 bp upstream of left TA continues into the complementary strand 44 bp downstream the right TA			1

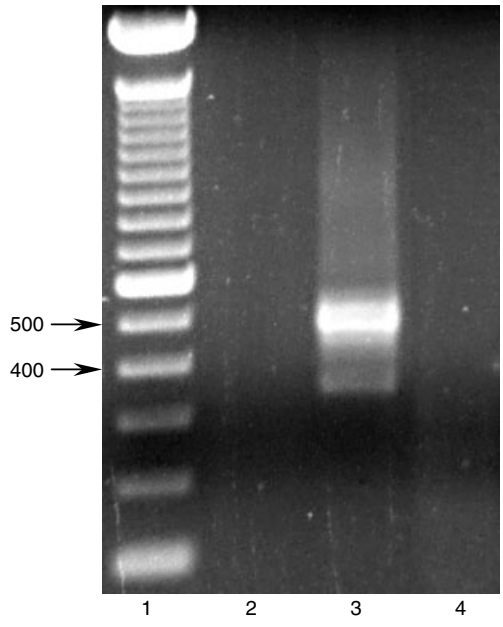

Figure 7. Excision products in the livers of SB-transposon-treated MPS VII mice. Lane 1, 100-bp interval markers; lane 2, treatment with pT/CAGGS-GUSB alone; lane 3, treatment with pT/CAGGS-GUSB + pCMVSB, lane 4, sham-treatment with pBluscript

recombination that did not use SB transposase. Taken together, the data suggest that the excision assay is useful for quickly evaluating transposition of transgenes into organs and tissues of living animals.

Discussion

We developed a plasmid-based excision assay for *Sleeping Beauty* (SB)-mediated transposition and confirm preliminary findings that suggested that excision rates correlate to transposition rates. Here we have used the excision assay as a simplified method to determine the outcome of the multi-step transposition process and to facilitate our understanding of the *cis*-elements required for SB excision. This PCR-based excision assay is independent of the transposon content and has shown that the excision assay can be used to monitor transposition in systems wherein drug selection is not feasible, such as in non-dividing cells of whole animal tissues. Thus, the excision assay offers a high-throughput means to detect and measure transposition in somatic tissues in which multiple transposition events occur in a large number of cells.

The excision assay was used to elucidate several parameters of transposition that have not been appreciated before. The first involves footprints left in the excision site. The ability to revert the transposition event after remobilization of the transposon is one potential advantage of using transposable elements in functional genomics. Consequently, it is important to know whether the footprint left after excision would maintain the open reading frame for translation. Two previous studies have provided conflicting results regarding the SB footprint. Luo *et al*. [14] observed canonical footprints in mouse embryonic stem cells, whereas Fischer *et al*. [4] observed non-canonical footprints in mouse haploid spermatids. In this study, we determined the footprints in tissue-cultured cells and whole animals. As summarized in Table 3, in HeLa cells there is a mixture of canonical footprints and non-canonical footprints. In zebrafish, mouse embryonic stem cells and mouse liver cells, most footprints are canonical. In haploid spermatids, none of the footprints were canonical. Together, these results show that SB leaves different footprints in different cell types and that the ability

to revert to wild type after remobilization may be limited by the cell or tissue type. In zebrafish embryos, and mouse embryonic stem cells and cells of the adult liver, 90% of the footprints add 5 bp (TA + CAG or CTG) to the open reading frame, which should cause a frame shift. In mouse haploid spermatids, over 40% of the footprints add only 3 bp, which would allow reversion to the wild-type phenotype. Thus, for experimental studies, reversion to wild type would be rare when using SB in zebrafish embryos, mouse embryonic stem cells, and tissues in mice. The footprint data also showed that when GG replaced the TA outside the outer DR, the substitution remained in the footprints. This supports the current model that the TA nucleotides flanking the transposon are not part of the transposon and are not carried over into a target site.

Double-strand breaks generated by transposon excision are thought to be repaired by a process called non-homologous end-joining [4]. In vertebrates, this process is catalyzed by a group of enzymes including Ku70 and Ku80 end-binding factors, the catalytic subunit of DNA-dependent protein kinase (DNA-PK), and the XRCC4/DNA ligase IV heteromeric complex. Mutation studies in yeast have shown that loss of different subsets of these enzymes leads to different repair products, including accurate repair, inaccurate repair, and a mixture of accurate and inaccurate repair [24]. These results resemble the different footprint patterns we observed in different cell types – mostly canonical footprints in zebrafish cells as well as mouse embryonic stem cells and liver cells, non-canonical footprints in mouse haploid spermatids, and a mixture of canonical and non-canonical footprints in HeLa cells. We suspect that the DNA repair machineries differ in some way that leaves characteristic footprints for each cell type. This hypothesis could be further investigated by examining SB footprints in cell lines with known repair defects.

The excision step we studied here is one of the major steps involved in transposition. Studies from other DNA transposons such as Tn10, Tn5 and Mu have identified the detailed steps of transposition. Specifically, excision of the transposon consists of transposase-binding to the terminal repeats followed by formation of a synaptic complex comprising the transposon–transposase. For the Mu transposon, this step is called transpososome assembly. The cut-and-paste reaction then occurs with first-strand nicking, hairpin formation and hairpin resolution, which releases the transposon from the donor site, and marks the end of the excision step. Biochemical studies in these systems have shown that the terminal nucleotides at the transposon-donor junction are involved in steps subsequent to DNA binding but before excision. In Mu, the terminal nucleotides at the transposon-junction sequences are involved in transpososome assembly [26,27]. In Tn5, the end sequences are specifically required for synaptic complex formation [28]. In Tn10, mutations in these nucleotides prevent hairpin formation and strand transfer [25]. In SB-mediated transposition, mutations in terminal nucleotides do not affect transposase binding, but do affect excision activity, indicating they may have a similar function subsequent to DNA binding but before excision as with other DNA transposons.

Our study of nucleotides bordering the sites of excision both inside and outside the transposon suggests that the requirement of transposon-donor junction nucleotides for excision is not base-pair specific. Replacement of the TA-dinucleotide, or of single nucleotides at the end of the transposon, reduced but did not abolish excision activity. These nucleotides may work synergistically. Whereas point mutation at either position 1 or 3 at the end of the left IR reduced relative excision activity to 11 and 18%, respectively, the double mutation reduced the relative excision activity below the detectable limit, about 5% ($11\% \times 18\% < 5\%$). These results suggest that the nucleotides in this region may contribute to a certain environment to affect transposon–transposase interactions. This environment could have certain physical properties required for transposase catalytic activity, similar to the one observed at the target site [15,17; G. Liu, in preparation]. Perturbing these interactions would result in a less favorable environment that would lead to a decrease in the rate of excision and an approximately equal decrease in the rate of transposition. If this hypothesis is true, then the flanking sequence of the transposon outside the TA-dinucleotides might influence transposon activity as well. Thus, with the excision assay, we should be able to improve further the flanking sites, which, like improving the activity of SB transposase [13], should lead to more a more powerful transposon system.

Our results have considerable potential for developing non-viral, transposon-mediated, gene-transfer vectors for human therapy. At present, the only method for evaluation of transposition events in organs of multi-cellular animals is to sequence insertion sites in chromosomes of treated animals because each cell in which the transposon integrates is a separate event that is non-clonal. This procedure is exceptionally labor-intensive and non-quantitative. In contrast, by employing the excision assay a few days after gene transfer, investigators will be able to approximate efficiently and quickly the levels of transposition into chromosomes of a multi-cellular organ. Thus, the excision assay should be extremely useful for evaluation of parameters affecting gene delivery using plasmids as donor vehicles.

Acknowledgements

We thank Dr. Akihiko Koga and Dr. Koichi Kawakami for assistance in development of the excision assay. We are especially grateful to Dr. Yusuke Kamachi and Heather Gardner for instructive discussions. Many thanks to Stephen Ekker, Scott McIvor, David Largaespada and other members of the Beckman Center for Transposon Research for insights and guidance and David Erickson for help with the manuscript and tables. This work was supported by grants from the Arnold and Mabel Beckman Foundation and the NIH (NCRR R01-066525-07 and NICHD P01-HD32652). ELA was supported by a Viking Children's Fund Grant-in-Aid.

References

1. Plasterk RH. The Tc1/mariner transposon family. *Curr Top Microbiol Immunol* 1996; **204**: 125–143.
2. Plasterk RH, Izsvak Z, Ivics Z. Resident aliens: the Tc1/mariner superfamily of transposable elements. *Trends Genet* 1999; **15**: 326–332.
3. Ivics Z, Hackett PB, Plasterk RH, Izsvak Z. Molecular reconstruction of Sleeping Beauty, a Tc1-like transposon from fish, and its transposition in human cells. *Cell* 1997; **91**: 501–510.
4. Fischer SE, Wienholds E, Plasterk RH. Regulated transposition of a fish transposon in the mouse germ line. *Proc Natl Acad Sci U S A* 2001; **98**: 6759–6764.
5. Izsvak Z, Ivics Z, Plasterk RH. Sleeping Beauty, a wide host-range transposon vector for genetic transformation in vertebrates. *J Mol Biol* 2000; **302**: 93–102.
6. Dupuy AJ, Fritz S, Largaespada DA. Transposition and gene disruption in the male germline of the mouse. *Genesis* 2001; **30**: 82–88.
7. Horie K, Kuroiwa A, Ikawa M, *et al*. Efficient chromosomal transposition of a Tc1/mariner-like transposon Sleeping Beauty in mice. *Proc Natl Acad Sci U S A* 2001; **98**: 9191–9196.
8. Clark KJ, Geurts AM, Bell JB, Hackett PB. Transposon vectors for gene-trap insertional mutagenesis in vertebrates. *Proc Natl Acd Sci U S A* 2003; submitted.
9. Dupuy AJ, Clark KJ, Carlson CM, *et al*. Mammalian germ-line transgenesis by transposition. *Proc Natl Acad Sci U S A* 2002; **99**: 4495–4499.
10. Yant SR, Meuse L, Chiu W, *et al*. Somatic integration and long-term transgene expression in normal and haemophilic mice using a DNA transposon system. *Nat Genet* 2000; **25**: 35–41.
11. Yant SR, Ehrhardt A, Mikkelsen JG, *et al*. Transposition from a gutless adenotransposon vector stabilizes transgene expression in vivo. *Nat Biotechnol* 2002; **20**: 999–1005.
12. Belur LR, Frandsen JL, Dupuy AJ, *et al*. Gene insertion and long-term expression in lung mediated by the *Sleeping Beauty* transposon system. *Mol Ther* 2003; **8**: 501–507.
13. Geurts AM, Yang Y, Clark KJ, *et al*. Gene transfer into genomes of human cells by the *Sleeping Beauty* transposon system. *Mol Ther* 2003; **8**: 108–117.
14. Luo G, Ivics Z, Izsvak Z, Bradley A. Chromosomal transposition of a Tc1/mariner-like element in mouse embryonic stem cells. *Proc Natl Acad Sci U S A* 1998; **95**: 10 769–10 773.
15. Vigdal TJ, Kaufman CD, Izsvak Z, *et al*. Common physical properties of DNA affecting target site selection of *Sleeping Beauty* and other Tc1/*mariner* transposable elements. *J Mol Biol* 2002; **323**: 441–452.
16. Cui Z, Geurts AM, Liu G, *et al*. Structure-function analysis of the inverted terminal repeats of the *Sleeping Beauty* transposon. *J Mol Biol* 2002; **318**: 1221–1235.
17. Izsvak Z, Khare D, Behlke J, *et al*. Involvement of a bifunctional, paired-like DNA-binding domain and a transpositional enhancer in Sleeping Beauty transposition. *J Biol Chem* 2002; **277**: 34 581–34 588.
18. Kawakami K, Koga A, Hori H, Shima A. Excision of the tol2 transposable element of the medaka fish, *Oryzias latipes*, in zebrafish. *Danio rerio. Gene* 1998; **225**: 17–22.
19. Kawakami K, Shima A. Identification of the Tol2 transposase of the medaka fish *Oryzias latipes* that catalyzes excision of a nonautonomous Tol2 element in zebrafish *Danio rerio*. *Gene* 1999; **240**: 239–244.
20. Available: http://www.cbs.umn.edu/labs/perry/.
21. Liu F, Song YK, Liu D. Hydrodynamics-based transfection in animals by systemic administration of plasmid DNA. *Gene Ther* 1999; **6**: 1258–1266.
22. Zhang G, Budker V, Wolff JA. High levels of foreign gene expression in hepatocytes after tail vein injections of naked plasmid DNA. *Hum Gene Ther* 1999; **10**: 1735–1737.
23. Birkenmeier EH, Davisson MT, Bearner WG, *et al*. Murine mucopolysaccharidosis VII: characterization of a mouse with β-glucuronidase deficiency. *J Clin Invest* 1989; **83**: 1258–1266.
24. Critchlow SE, Jackson SP. DNA end-joining: from yeast to man. *Trends Biochem Sci* 1998; **23**: 394–398.
25. Allingham JS, Wardle SJ, Haniford DB. Determinants for hairpin formation in Tn10 transposition. *EMBO J* 2001; **20**: 2931–2942.
26. Coros CJ, Chaconas G. Effect of mutations in the Mu-host junction region on transpososome assembly. *J Mol Biol* 2001; **310**: 299–309.
27. Lee I, Harshey RM. Importance of the conserved CA dinucleotide at Mu termini. *J Mol Biol* 2001; **314**: 433–444.
28. Bhasin A, Goryshin IY, Steiniger-White M, *et al*. Characterization of a Tn5 pre-cleavage synaptic complex. *J Mol Biol* 2000; **302**: 49–63.